Article

Determining the influence of endoskeleton friction on the damping of pulsating antibubbles

Anderton, Nicole, Carlson, Craig S., Aharonson, Vered and Postema, Michiel

Anderton, Nicole, Carlson, Craig S., Aharonson, Vered and Postema, Michiel (2022) Determining the influence of endoskeleton friction on the damping of pulsating antibubbles. Current Directions in Biomedical Engineering, 8 (2). pp. 781-784. ISSN 2364-5504

It is advisable to refer to the publisher's version if you intend to cite from the work.
http://dx.doi.org/10.1515/cdbme-2022-1199

Nicole Anderton*, Craig S. Carlson, Vered Aharonson, and Michiel Postema

Determining the influence of endoskeleton friction on the damping of pulsating antibubbles

https://doi.org/10.1515/cdbme-2022-1199

Abstract: Recent *in-vivo* work showed the suitability of Pickering-stabilized antibubbles in harmonic imaging and ultrasound-guided drug delivery. To date, however, theoretical considerations of antibubble core properties and their effects on antibubble dynamics have been rather sparse. The purpose of this study was to investigate the influence of skeletal friction on the damping of a pulsating antibubble and the pulsation phase of an antibubble relative to the incident sound wave. Numerical simulations were performed to compute damping terms and pulsation phases of micron-sized antibubbles with thin elastic shells and 30% endoskeleton volume fraction. The simulations showed that the damping owing to skeleton presence dominates the damping mechanism for antibubbles of radii less than 2.5 μm, whilst it is negligible for greater radii. The pulsation phase of such small antibubbles was simulated to have a phase delay of up to $\frac{1}{6}\pi$ with respect to pulsating free gas bubbles. Our findings demonstrate that the presence of an endoskeleton inside a bubble influences pulsation phase and damping of small antibubbles. Antibubbles of radii less than 3 μm are of interest for the use as ultrasound contrast agents.

Keywords: Acoustic driving, ultrasound contrast agent, endoskeleton, antibubble damping modelling, harmonic oscillation.

1 Introduction

Endoskeletal antibubbles comprise gas bubbles with one or more liquid cores. These cores are suspended by a solid skeletal structure consisting of hydrophobic particles [1], as shown in Figure 1.

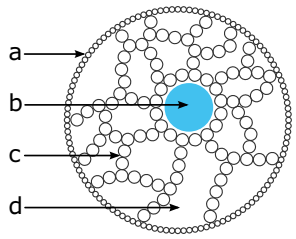

Fig. 1: Microscopic photograph of an endoskeletal antibubble and a schematic representation thereof: (a) shell; (b) liquid core; (c) skeleton; (d) gas.

As free, unencapsulated, antibubbles, are short-lived [2–5], antibubbles are typically stabilized by adsorbing nanoparticles to the liquid–gas interfaces. This process has been referred to as Pickering-stabilizing [6].

When subjected to ultrasound, the presence of an incompressible core allows for asymmetric pulsation excursions, even at modest acoustic driving amplitudes [7]. Consequently, antibubbles have been proposed as ultrasound contrast agents for low-mechanical-index harmonic imaging [8, 9]. If the liquid cores are loaded with therapeutics, antibubbles act as vehicles for ultrasound-guided drug delivery, as shown recently *in vivo* [10].

For diagnostic as well as therapeutic applications, it is highly relevant to predict antibubble dynamics and to quantify the influence of the presence of liquid and solid cores on these dynamics. In this study, we investigated the influence of skeletal friction on the pulsation phase of an antibubble relative to the incident sound wave. The purpose of this investigation was to quantify the core presence from pulsation phase observations.

Pulsation phases of damped oscillators have been analyzed thoroughly for forced mass–spring–dashpot systems [11]. They had been simulated for pulsating ultrasound contrast agent microbubbles with various shell thicknesses [12, 13]. Pulsation phases of antibubbles have not been previously reported on.

Radial pulsations of shell-encapsulated microbubbles have been modeled using adaptations of the Rayleigh-Plesset equation. These have been modified to account for specific

***Corresponding author: Nicole Anderton,** BioMediTech, Faculty of Medicine and Health Technology, Tampere University, Korkeakoulunkatu 3, 33720 Tampere, Finland, e-mail: nicole.anderton@tuni.fi
Craig S. Carlson, Michiel Postema, BioMediTech, Faculty of Medicine and Health Technology, Tampere University, Tampere, Finland and School of Electrical and Information Engineering, University of the Witwatersrand, Johannesburg, Braamfontein, South Africa
Vered Aharonson, School of Electrical and Information Engineering, University of the Witwatersrand, Johannesburg, Braamfontein, South Africa and School of Sciences, University of Central Lancashire — Cyprus, Pyla, Cyprus and Afeka Tel Aviv Academic College of Engineering, Tel Aviv, Israel

properties of the surrounding medium, for high-amplitude acoustic driving [14], for changes in surface tension owing to buckling [15], for the presence of a solid elastic shell [16], a thin lipid shell [17], a viscous or viscoelastic shell [18, 19], for the presence of another oscillator nearby [20], and for tethering [21], just to name a few. Several review articles have been dedicated to comparing the many models [22–24]. In principle, the most basic Rayleigh-Plesset equation suffices for a precise estimation of the radial dynamics of a shell-encapsulated microbubble, provided that the pulsation velocity does not approach the speed of sound, the pulsation excursion amplitude is much less than the resting size, and only few pulsation cycles are taken into account, so that viscous or viscoelastic effects remain negligible. In this study, we were assuming low-amplitude very short-pulsed ultrasound, which justifies our choice for a rather simplistic model.

In previous simulation studies, the combined solid and liquid internal structure had been represented by an incompressible volume $V_c = \varphi V_0$, where $\varphi \in [0,1\rangle$ is the constant volume fraction and V_0 is the volume of the antibubble [7]. Empirical evidence to justify a constant size-independent volume fraction exists in the form of scanning electron microscopy and confocal microscopy images [1].

2 Theory

Let us consider an antibubble of resting radius R_0 with an infinitesimal shell and surrounded by an infinite liquid of density ρ. If the antibubble is forced by a short short pressure pulse $p(\omega t)$ of angular center frequency ω, whose amplitude is so small that that the pulsation amplitude of the antibubble is less than R_0, we may regard this system as a forced damped oscillator with an effective mass $m = 4\pi\rho(R_0+x)^3$ [25], instantaneous excursion x, damping coefficient δ [25, 26], and angular resonance frequency ω_r.

If the amplitude of the driving function function is instantly lessened [27], the damping coefficient of the pulsating entity undergoing damping can then be determined by measuring two consecutive decaying excursion amplitudes x_i and x_{i+1} (*cf.* Figure 2) and substituting them into [11]:

$$\delta = \frac{2\ln\frac{x_i}{x_{i+1}}}{(2\pi)^2 + \left(\ln\frac{x_i}{x_{i+1}}\right)^2} \,. \tag{1}$$

We propose that, for an endoskeletal antibubble, the damping coefficient consists of five components, four of which are identical to those of shell-encapsulated microbubbles:

$$\delta = \delta_v + \delta_r + \delta_{\textcircled{\scriptsize}} + \delta_{\textcircled{\scriptsize}} + \delta_\theta \,, \tag{2}$$

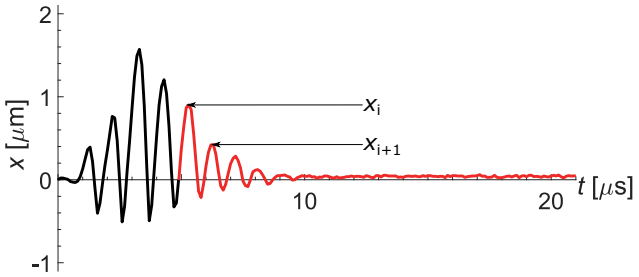

Fig. 2: Antibubble excursion as a function of time, for an antibubble of resting radius $R_0 = 5\,\mu$m, forced by a short pulse. The unforced pulsation part is represented by a red line.

where

$$\delta_v = \frac{4\eta}{\omega\rho\,(R_0+x)^2} \tag{3}$$

is the viscous damping [26], in which η is the dynamic viscosity of the surrounding medium,

$$\delta_r = \frac{\omega\,(R_0+x)}{c} \tag{4}$$

is the damping owing to reradiation [26], in which c is the speed of sound of the surrounding medium,

$$\delta_{\textcircled{\scriptsize}} = \frac{S_{\textcircled{\scriptsize}}}{m\,\omega} \tag{5}$$

is the damping owing to friction in the shell, in which $S_{\textcircled{\scriptsize}}$ is the outer shell friction parameter [28],

$$\delta_{\textcircled{\scriptsize}} = \varphi^n \frac{S_{\textcircled{\scriptsize}}}{m\,\omega} \tag{6}$$

is the damping owing to friction in the endoskeleton, in which n is a noninteger power and $S_{\textcircled{\scriptsize}}$ is a thus-far undefined skeleton friction parameter, and

$$\delta_\theta = \frac{\frac{\sinh X+\sin X}{\cosh X-\cos X} - \frac{2}{X}}{\frac{X}{3(\gamma-1)} + \frac{\sinh X+\sin X}{\cosh X-\cos X}} \left(\frac{\omega_r}{\omega}\right)^2 \tag{7}$$

is the thermal damping, in which $X = \frac{R_0}{l_D}\left(1-\varphi^{\frac{1}{3}}\right) > 1$. The thermal boundary layer thickness is given by Eller [29]:

$$l_D = \sqrt{\frac{K_g}{2\,\omega\,\rho_g\,C_p}} \,, \tag{8}$$

where C_p is the specific heat of the gas, K_g is the thermal conductivity of the gas, ρ_g is the density of the gas.

An expression for the linear angular resonance frequency of a shell-encapsulated antibubble has been stated by Kudo [1]. A derivation of the difference in pulsation phase of any base-forced damped oscillator was shown by Attenborough and Postema [11]. A solution for a single bubble structure was presented by Postema and Schmitz [13]:

$$\alpha = \pi + \arctan\left(\frac{\left(\frac{\omega}{\omega_r}\right)\delta}{1-\left(\frac{\omega}{\omega_r}\right)^2}\right) \,, \tag{9}$$

where α is the phase difference between the antibubble pulsation and the incident sound field.

3 Methods

Numerical solutions of (2)–(9) were computed using MATLAB®. The input parameters were chose such that they simulated experimental situations in antibubble literature: $c = 1480\,\mathrm{m\,s^{-1}}$, $C_\mathrm{p} = 1000\,\mathrm{J\,kg^{-1}\,K^{-1}}$, $K_\mathrm{g} = 0.025\,\mathrm{W\,m^{-1}\,K^{-1}}$, $\eta = 1.00\,\mathrm{mPa}$, $\rho = 998\,\mathrm{kg\,m^{-3}}$, $\rho_\mathrm{g} = 1.00\,\mathrm{kg\,m^{-3}}$, $\sigma = 0.072\,\mathrm{N\,m^{-1}}$, $\omega = 2\pi \times 1.0 \times 10^6\,\mathrm{s^{-1}}$. The outer shell was considered of negligible stiffness $\leq 0.2\,\mathrm{N\,m^{-1}}$.

During our simulations, the expression $\left(S_{\text{◔}} + \varphi^n S_{\text{※}}\right)$ was treated as a single variable.

The resting radius was varied from 0.5 μm to 12 μm.

4 Results and discussion

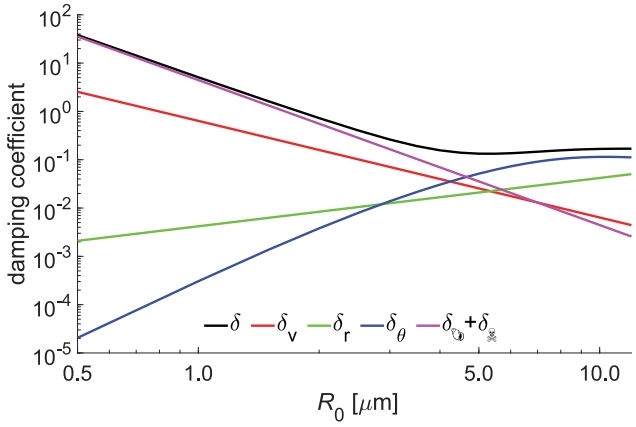

Fig. 3: Dimensionless damping coefficient and its contributing components as a function of antibubble resting radius.

Figure 3 shows the damping coefficient and its contributing components for an antibubble with an endoskeleton of 30% volume fraction. The shell friction and skeleton friction parameters had been chosen conservatively, with equal values of 0.27 $\mu\mathrm{N\,s\,m^{-1}}$, similar to some lipids. For greater values, the damping was observed to be dominated by thermal damping and reradiation. For antibubbles of resting radii less than 2.5 μm, however, the damping owing to shell and endoskeleton presence was even greater than the viscous damping term. The trade-off size coincided with the resonant size at the driving frequency of 1 MHz. It is noted that antibubbles with greater volume fraction have an even stronger skeleton friction damping term (not shown). As ultrasound contrast agent particles need to have diameters less than those of capillaries, the findings of the smaller antibubbles are most relevant to medical imaging.

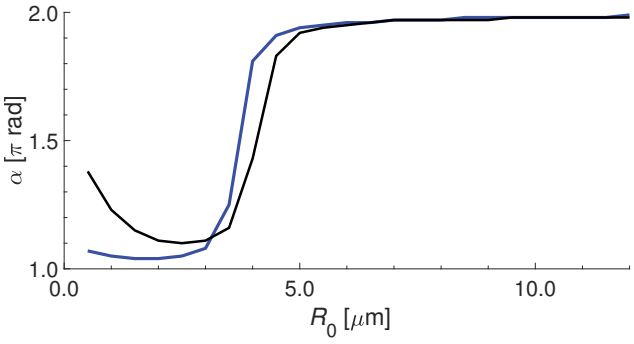

Fig. 4: Pulsation phase with respect to the incident sound field, as a function of resting radius, for an antibubble (black) and a free gas bubble (blue).

Figure 4 shows the pulsation phase of an antibubble and a free gas bubble, with respect to an incident pulse of 1-MHz central driving frequency. At the parameters chosen, only the smaller antibubbles were found to have a substantially different pulsation phase compared tot the free gas bubbles. A phase difference of up to $\frac{1}{6}\pi$ was computed. The finding is useful in optically or acoustically determining whether a bubble is a core-comprising antibubble or an empty gas bubble.

5 Conclusions

Pulsation phases of micron-sized antibubbles differed from those of free gas bubbles. These differences may be attributed to the friction of the antibubble shells and skeletons.

For smaller antibubbles, shell and skeleton friction were found to be the dominant damping mechanisms of pulsating antibubbles driven at frequencies less than their resonance frequencies.

Author statement

Research funding: This work was supported by the National Research Foundation of South Africa, Grant Numbers 97742 and 127102, and by the Academy of Finland, Grant Number 340026. Conflict of interest: Authors state no conflict of interest. Informed consent: Authors state that informed consent is not applicable. Ethical approval: Authors state that no ethical approval was required for this research as no human or animal samples or data were used.

References

[1] Kudo N, Uzbekov R, Matsumoto R, Shimizu R, Carlson CS, Anderton N, et al. Asymmetric oscillations of endoskeletal antibubbles. Jpn J Appl Phys 2020;59:SKKE02.

[2] Dorbolo S, Caps H, Vandewalle N. Fluid instabilities in the birth and death of antibubbles. New J Phys 2003;5:161.

[3] Postema M, ten Cate FJ, Schmitz G, de Jong N, van Wamel A. Generation of a droplet inside a microbubble with the aid of an ultrasound contrast agent: first result. Lett Drug Des Discov 2007;4:74–77.

[4] Vitry Y, Dorbolo S, Vermant J, Scheid B. Controlling the lifetime of antibubbles. Adv Colloid Interfac Sci 2019;270:73–86.

[5] Zou J, Ji C, Yuan BG, Ruan XD, Fu X. Collapse of an antibubble. Phys Rev E 2013;87:061002.

[6] Poortinga AT. Long-lived antibubbles: stable antibubbles through Pickering stabilization. Langmuir 2011;27:2138–2141.

[7] Kotopoulis S, Johansen K, Gilja OH, Poortinga AT, Postema M. Acoustically active antibubbles. Acta Phys Pol A 2015;127:99–102.

[8] Postema M, Novell A, Sennoga C, Poortinga AT, Bouakaz A. Harmonic response from microscopic antibubbles. Appl Acoust 2018;137:148–150.

[9] Panfilova A, Chen P, van Sloun RJG, Wijkstra H, Postema M, Poortinga AT, et al. Experimental acoustic characterization of an endoskeletal antibubble contrast agent: first results. Med Phys 2021;48:6765–6780.

[10] Kotopoulis S, Lam C, Haugse R, Snipstad S, Murvold E, Jouleh T, et al. Formulation and characterisation of drug-loaded antibubbles for image-guided and ultrasound-triggered drug delivery. Ultrason Sonochem 2022;105986.

[11] Attenborough K, Postema M. A pocket-sized introduction to dynamics. Kingston upon Hull: University of Hull 2008.

[12] Postema M, de Jong N, Schmitz G. The physics of nanoshelled microbubbles. Biomed Tech 2005;50(S1):748–749.

[13] Postema M, Schmitz G. Ultrasonic bubbles in medicine: influence of the shell. Ultrason Sonochem 2007;14:438–444.

[14] Frinking P, de Jong N, Cespedes I. Scattering properties of encapsulated gas bubbles at high ultrasound pressures. J Acoust Soc Am 1999;105:1989–1996.

[15] Marmottant P, van der Meer S, Emmer M, Versluis M, de Jong N, Hilgenfeldt S, et al. A model for large amplitude oscillations of coated bubbles accounting for buckling and rupture. J Acoust Soc Am 2005;118:3499–3505.

[16] Church CC. The effects of an elastic solid surface layer on the radial pulsations of gas bubbles. J Acoust Soc Am 1995;97:1510–1521.

[17] Doinikov AA, Dayton PA. Maxwell rheological model for lipid-shelled ultrasound microbubble contrast agents. J Acoust Soc Am 2007;121:3331–3340.

[18] Sarkar K, Shi WT, Chatterjee D, Forsberg F. Characterization of ultrasound contrast microbubbles using in vitro experiments and viscous and viscoelastic interface models for encapsulation. J Acoust Soc Am 2005;118:539–550.

[19] Tsiglifis K, Pelekasis NA. Nonlinear radial oscillations of encapsulated microbubbles subject to ultrasound: the effect of membrane constitutive law. J Acoust Soc Am 2008;123:4059–4070.

[20] Doinikov AA. Equations of coupled radial and translational motions of a bubble in a weakly compressible liquid. Phys Fluids 2005;17:128101.

[21] Maksimov A, Leighton T, Birkin P. Dynamics of a tethered bubble. AIP Conf Proc 2006;838:512.

[22] Vokurka K. Comparison of Rayleigh's, Herring's, and Gilmore's models of gas bubbles. Acustica 1986;59:214–219.

[23] Doinikov AA, Bouakaz A. Review of shell models for contrast agent microbubbles. IEEE Trans Ultrason Ferroelectr Freq Control 2011;58:981–993.

[24] Versluis M, Stride E, Lajoinie G, Dollet B, Segers T. Ultrasound contrast agent modeling: a review. Ultrasound Med Biol 2020;46:2117–2144.

[25] Medwin H. Counting bubbles acoustically: a review. Ultrasonics 1977;15:7–13.

[26] Devin C. Survey of thermal, radiation, and viscous damping of pulsating air bubbles in water. J Acoust Soc Am 1959;31:1654–1667.

[27] Leighton TG, White PR, Morfey CL, Clarke JWL, Heald GJ, Dumbrell HA, Holland KR. The effect of reverberation on the damping of bubbles. J Acoust Soc Am, 2002;112:1366–1376.

[28] de Jong N, Cornet R, Lancée CT. Higher harmonics of vibrating gas-filled microspheres. Part one: simulations. Ultrasonics 1993;32:447–453.

[29] Eller AI. Damping constants of pulsating bubbles. J Acoust Soc Am 1970;47:1469–1470.